Geophysical Journal (1988) **94**, 295–307

Vectorial tomography – I. Theory

Jean-Paul Montagner[1] and Henri-Claude Nataf[2]

[1] *Laboratoire de Sismologie, Institut de Physique du Globe, 4 Place Jussieu, 75230 Paris, France*
[2] *Laboratoire de Geodynamique interne, Universite Paris-Sud, 91405 Orsay, France*

Accepted 1988 January 26. Received 1988 January 26; in original form 1986 July 9

SUMMARY

By inverting the azimuthal dependence of Rayleigh and Love dispersions (including the azimuthally averaged term) it is possible to separate the effect of anisotropy from other effects creating lateral heterogeneities (mainly thermal). The different steps of the tomographic method are described. In the first step, we retrieve the geographical distributions of the different azimuthal dispersion terms of Rayleigh and Love waves. For a complete slightly anisotropic medium, these distributions are dependent upon 13 combinations of elastic moduli. This number of parameters is too large and in order to interpret these distributions as simply as possible in terms of elastic properties of the medium, some realistic assumptions about the material can be made. The simplest way to explain the azimuthal distributions is to assume that the medium possesses a symmetry axis but contrarily to previous investigations, it is assumed that the orientation of this axis is not necessarily vertical. In that case, one shows how to retrieve simultaneously the 3-dimensional distributions of seismic velocities and of anisotropy characterized as a vector by an amplitude and the two angles of the symmetry axis. This complete process has been named 'vectorial tomography' and can provide valuable information about convection and also mineralogical composition.

Key words: Anisotropy, orthotropy, petrological models, tomography

INTRODUCTION

The seismic surface wave tomographic models on a global scale (Woodhouse & Dziewonski 1984; Nataf, Nakanashi & Anderson 1984, 1986; Tanimoto & Anderson 1985; Tanimoto 1986a,b) displayed the location of S-wave velocity heterogeneities in the Earth's mantle. By including Love wave dispersion, Nataf *et al.* (1984, 1986) within the hypothesis of transverse isotropy with vertical symmetry axis, obtained the geographical distribution of the S-wave anisotropy at different depths, and they relate this kind of anisotropy to the orientation of the convective flow throughout the mantle. Tanimoto & Anderson (1984) obtained a global scale distribution of the Rayleigh wave azimuthal anisotropy in terms of spherical harmonics up to degree 4 by using R2 and R3 phases at different periods. They found a good correlation of fast Rayleigh wave directions with upper mantle return flow directions derived from kinematic considerations (Hager & O'Connell 1979). The azimuthal anisotropy most likely originates from the preferred orientation of olivine crystals (Nicolas & Poirier 1976) and can be related to the horizontal flow direction but so far, the simultaneous inversion at depth of Rayleigh and Love waves dispersion and their azimuthal dependence has not been performed.

From a theoretical point of view, Smith & Dahlen (1973) studied the effect of a slight elastic anisotropy on the propagation of Love and Rayleigh waves in a plane-layered medium. Crampin (1970) and Maupin (1985) also studied the propagation of surface waves in anisotropic plane-layered media and investigated a few special cases. Montagner & Nataf (1986), following the approach of Smith & Dahlen (1973), showed that only simple linear combinations of the elastic tensor coefficients are necessary to describe the total effect of anisotropy (both 'polarization' anisotropy and azimuthal anisotropy) on surface waves. The 'polarization' anisotropy, so-called by Schlue & Knopoff (1977) results from the inability to explain Love and Rayleigh dispersion by a simple isotropic model. In order to avoid a possible confusion between 'polarization' anisotropy and anomalies in the polarization of the particle motion induced by anisotropy, Mitchell (1984) proposed the term Love/Rayleigh incompatibility be used rather than 'polarization' anisotropy. The 'polarization' anisotropy displayed by Montagner & Nataf (1986) correspond to the $0-\psi$ term of their azimuthal expansion describing the equivalent transversely isotropic medium with vertical symmetry axis. They propose a simple method for retrieving the anisotropy at depth and they calculate for a spherical Earth the partial derivatives needed for performing the inversion.

In this first paper we address the question of the inversion of a complete dataset of surface-wave group or phase velocities including different azimuthal terms and we investigate what information can be derived about lateral heterogeneities of seismic velocities and anisotropy. The tomographic method as a first step provides the geographical

* Present address: Seismological Laboratory, California Institute of Technology, Pasadena, CA 91125, USA.

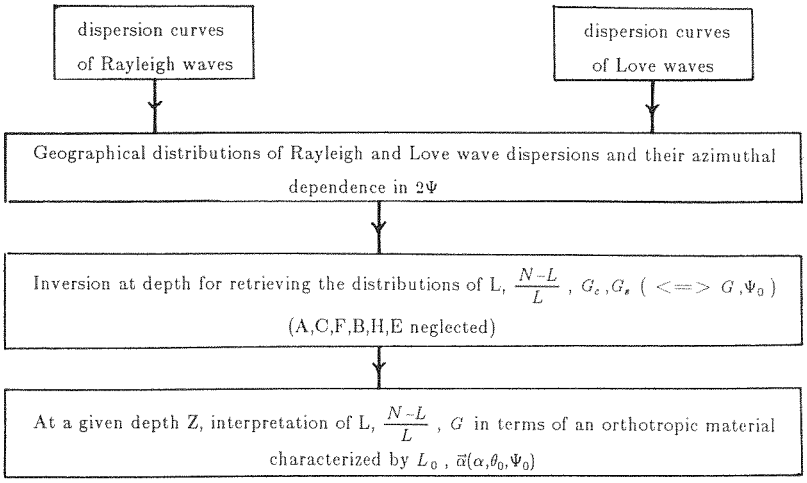

Figure 1 General scheme of processing for 'Vectorial Tomography'.

distributions of the anisotropic combinations derived by Montagner & Nataf (1986). It is shown that a simple way to explain these consists in assuming that the material possesses a symmetry axis (orthotropic medium). This symmetry axis can be characterized by two angles and the difference of velocities between that in the direction of the symmetry axis and that in the perpendicular plane measures the amplitude of the anisotropy. Therefore the anisotropy of the medium can be described by a pseudo-vector (amplitude +2 angles) and the complete tomographic process is named 'Vectorial Tomography'. The complete procedure is summarized in Fig. 1 and we will consider successively its different steps.

INVERSION TECHNIQUE

In this section, we detail the different steps which lead to the retrieval of anisotropy as explained in terms of an orthotropic material with a symmetry axis of any orientation. Tomographic techniques for the upper mantle using surface waves invert primarily the dispersion properties of surface waves (Nataf *et al.* 1984, 1986; Tanimoto & Anderson 1985; Tanimoto 1986a; Suetsugu & Nakanishi 1985). A two-step procedure is generally used: First of all, the velocities along the paths are expanded on the basis of spherical harmonics and then this expansion is inverted at depth in order to find the three-dimensional structure of S-wave velocity. Woodhouse & Dziewonski (1984) use a different method by inverting the waveform data, but in order to retrieve the S-wave velocity heterogeneities, they use basically the phase information, not the amplitude information.

Montagner (1986a) also developed a two-step procedure but rather than expanding the unknown function on a basis of functions, he takes the function itself as the unknown, following the approach of Tarantola & Valette (1982). In this case, it is necessary to introduce a covariance function of spatial parameters characterized by an *a priori* uncertainty and a correlation length. The theoretical background has already been explained in previous papers (Tarantola & Valette 1982; Montagner 1986a; Montagner & Nataf 1986). Therefore we will only recall the equations necessary for the general process, but detail the complexity introduced by the simultaneous inversion of Rayleigh, Love azimuthally averaged velocities and their azimuthal dependence and the interpretation of the anisotropic elastic combinations provided by the inversion.

Forward problem

The forward problem consists in computing the local phase and group velocities of surface waves for a given spherical earth model and afterwards, by integrating these local dispersion velocities along a path, the theoretical dispersion curves can be calculated and compared to dispersion data.

Using Rayleigh's principle combined with the harmonic tensor decomposition of Backus (1970), Smith & Dahlen (1973) have shown that a slight elastic anisotropy gives rise to an azimuthal dependence of the local phase or group velocities of Love and Rayleigh waves of the form:

$$V(\omega, \psi) - V_0(\omega, \psi) = A_1(\omega) + A_2(\omega)\cos(2\psi) + A_3(\omega)\sin(2\psi) + A_4(\omega)\cos(4\psi) + A_5(\omega)\sin(4\psi). \quad (1)$$

Following the same approach but with a cartesian representation of the elastic tensor, Montagner & Nataf (1986) have shown that only simple combinations of the elastic coefficients are necessary to describe the total effect of anisotropy on surface waves in a plane-layered medium. Mochizuki (1986) applied Rayleigh's principle to compute the effect of anisotropy on the eigenfrequencies of free oscillations of the Earth. He decomposed the fourth-order elastic tensor by the use of the generalized spherical harmonics of Phinney & Burridge (1973). He showed that the eigenfrequency shift with respect to the reference model depends on 15 kernels and Wigner's 3-j symbols (Edmonds 1960). These kernels which are functions of latitude and longitude show that the eigenfrequency shift $\delta\omega$ depends at the same time on even and odd orders of lateral heterogeneities. But in the asymptotic case, odd terms are smaller by one order of magnitude than even terms. Also by using the asymptotic development of Wigner's 3-j symbols (Jordan 1978), it is easy to introduce the azimuth ψ along

the path and Tanimoto (1986b) showed that the asymptotic azimuthal dependence of $\Delta\omega$ is the same in a spherical earth as in a flat-layered medium. This last result justifies the hypothesis of Montagner & Nataf (1986) who assumed that the partial derivatives of the azimuthal terms with respect to the combinations of elastic coefficients (that they derived in the plane case) are proportional to the partial derivatives of a transversely isotropic earth in the case of a spherical earth.

We recall now the different combinations in terms of elastic parameters C_{ij} which are present in the different azimuthal terms $A_i(\omega)$ of equation (1) (Montagner & Nataf 1986): indices 1 and 2 refer to horizontal coordinates (1: direction of propagation) and index 3 refers to vertical coordinate.

Constant term (0ψ-azimuthal term)

(A_1)

$$A = \rho V_{PH}^2 = \frac{3}{8}(C_{11}+C_{22}) + \frac{1}{4}C_{12} + \frac{1}{2}C_{66}$$

$$C = \rho V_{PV}^2 = C_{33}$$

$$F = \frac{1}{2}(C_{13}+C_{23}) \qquad (2a)$$

$$L = \rho V_{SV}^2 = \frac{1}{2}(C_{44}+C_{55})$$

$$N = \rho V_{SH}^2 = \frac{1}{8}(C_{11}+C_{22}) - \frac{1}{4}C_{12} + \frac{1}{2}C_{66}$$

2ψ-azimuthal term:

(A_2)	(A_3)
$\cos 2\psi$	$\sin 2\psi$

$$B_c = \frac{1}{2}(C_{11}-C_{22}) \qquad B_s = C_{16}+C_{26}$$

$$G_c = \frac{1}{2}(C_{55}-C_{44}) \qquad G_s = C_{54} \qquad (2b)$$

$$H_c = \frac{1}{2}(C_{13}-C_{23}) \qquad H_s = C_{36}$$

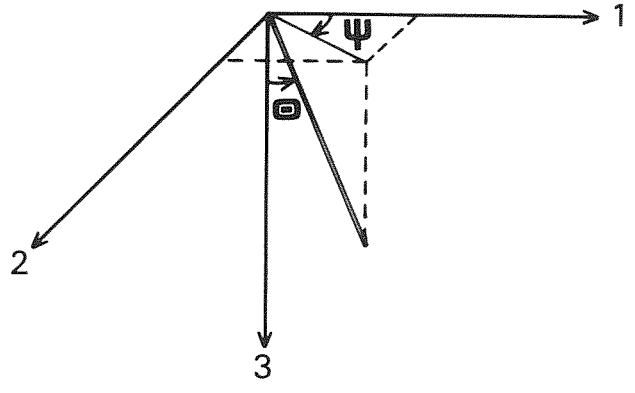

Figure 2 Definition of the angles θ and Ψ which characterize the symmetry axis of the material in a Cartesian coordinate system.

4ψ-azimuthal term:

(A_4)	(A_5)
$\cos 4\psi$	$\sin 4\psi$

$$E_c = \frac{1}{8}(C_{11}+C_{22}) - \frac{1}{4}C_{12} - \frac{1}{2}C_{66} \qquad E_s = \frac{1}{2}(C_{16}-C_{26}) \qquad (2c)$$

where ρ is the density, V_{PH}, V_{PV} are respectively horizontal and vertical P-wave velocities, V_{SH}, V_{SV} horizontal and vertical S-wave velocities.

From a practical point of view, it is very difficult to determine the 4ψ-azimuthal term because the azimuthal coverage must be quite good since the total variation occurs in only 45°. On the other hand, Montagner & Nataf (1986) computed the azimuthal variations of surface wave velocity that can be expected from a realistic elastic tensor for the upper mantle. They find that for Love waves, the contribution of $E_{c,s}$ to Rayleigh and Love waves 4ψ-anisotropy is small and much smaller than the contributions of $B_{c,s}$ and $G_{c,s}$ to the Rayleigh wave 2ψ-ansiotropy. One of the main conclusions of Montagner & Nataf (1986) is that the dominant azimuthal term is the 2ψ-azimuthal term of Rayleigh waves. Actually, this conclusion is valid if the upper mantle is primarily pyrolitic (Montagner & Anderson 1987). If the upper mantle is piclogitic (Anderson & Bass 1984) the 4ψ-azimuthal term of a Love wave can be almost as large as the 2ψ-azimuthal term of a Rayleigh wave.

On the other hand, Montagner & Nataf (1986) also point out that the 2ψ-azimuthal term at long periods can be explained either by shallow $B_{c,s}$ combinations or by deep $G_{c,s}$ combinations and that if we want to discriminate between shallow or deep anisotropy it is necessary to have as broad a period range for the data as possible. As we have no experience about these $B_{c,s}$ and $G_{c,s}$ combinations, *a priori* constraints on their variation range are not obvious. It must also be noted that this problem of discrimination between shallow $B_{c,s}$ or deep $G_{c,s}$ is exactly the same as the trade-off between shallow P-wave velocity and deep S-wave velocity anomalies in the inversion of dispersion data because the $B_{c,s}$ derivative is the same as the A-derivative related to P-wave $A = \rho V_{PH}^2$) and the $G_{c,s}$ derivative is the same as the L-derivative related to SV-wave ($L = \rho V_{SV}^2$). The $B_{c,s}$ combinations are the combinations that describe the 2ψ-azimuthal variation of P_n velocity (Backus 1965). Therefore, since many data are becoming available on the azimuthal variation of P_n velocities, we can hope that it will be possible to correct for this shallow effect in the future.

The measured velocity V_d can be related to the local velocity $V(M)$ in the geometrical optics approximation. This approximation is valid in the period range that we will consider (40–300 s) (Jordan 1978; Davis & Henson 1986). In taking account of the azimuthal dependence of the local velocity given by equation (1), we get:

$$\frac{\Delta}{V_d} = \int_{path} \frac{ds}{V(M)}$$

$$= \int_{path} \frac{ds}{V_0 + A_1(M,\omega) + A_2(M,\omega)\cos(2\psi) + A_3(M,\omega) \times \sin(2\psi) + A_4(M,\omega)\cos(4\psi) + A_5(M,\omega)\sin(4\psi)} \qquad (3)$$

As a first approximation, we can consider that the azimuthal terms $A_i(M, \omega)$ are first-order perturbations of the constant velocity V_0. Therefore, the forward problem can be stated as follows:

$$\begin{aligned}\frac{\Delta}{V_d}-\frac{\Delta}{V_0}(\omega)=&\int_{\text{path}}-A_1(M,\omega,\rho,A,C,F,L,N)\frac{ds}{V_0^2(\omega)}\\&-\int_{\text{path}}A_2(M,\omega,B_c,G_c,H_c)\cos 2\psi\frac{ds}{V_0^2(\omega)}\\&-\int_{\text{path}}A_3(M,\omega,B_s,G_s,H_s)\sin 2\psi\frac{ds}{V_0^2(\omega)}\\&-\int_{\text{path}}A_4(M,\omega,E_c)\cos 4\psi\frac{ds}{V_0^2(\omega)}\\&-\int_{\text{path}}A_5(M,\omega,E_s)\sin 4\psi\frac{ds}{V_0^2(\omega)}\end{aligned}\tag{4}$$

where Δ is the epicentral distance between the source and the receiver.

The different kernels which are present in A_i are explicitly stated in Montagner & Nataf (1986) and Tanimoto (1986b) and can be computed from the program of Dziewonski & Anderson (1981) computing the eigenfunctions of any transversely isotropic spherical earth model. We note again that to first order in anisotropy, the azimuthal dependence of Rayleigh and Love wave velocities is valid as well for phase velocity as for group velocity (Smith & Dahlen 1973).

The inverse method

As we know how to solve the forward problem and compute the different partial derivatives of data with respect to the parameters of a general slightly anisotropic medium, it is now possible to invert a given dataset for these parameters. We use the continuous form of the algorithm of Tarantola & Valette (1982) without either *a priori* regionalization or blocks. The notations of Tarantola & Valette (1982) and Montagner (1986a) are used throughout this section.

Let $\mathbf{p}(\mathbf{r})$ be a model of the earth. It is a set of unknown functions which could explain a set of observable quantities, the discrete dataset $\mathbf{d}$. It is assumed that a theory relating $\mathbf{d}$ and $\mathbf{p}$ exists: $\mathbf{d}=\mathbf{g}(\mathbf{p})$. This theory solves the forward problem.

Let $\mathbf{p}_0(\mathbf{r})$ be an *a priori* model and $\mathbf{d}_0$ the synthetic data such that $\mathbf{d}_0=\mathbf{g}(\mathbf{p}_0)$. Tarantola & Valette (1982) showed that in a least-squares sense, the solution of the inverse problem is given by:

$$\mathbf{p}(\mathbf{r})=\mathbf{p}_0(\mathbf{r})+\tilde{G}^{-1}[\mathbf{d}-\mathbf{g}(\mathbf{p})+G(\mathbf{p}-\mathbf{p}_0)]\tag{5a}$$

where $\tilde{G}^{-1}$ is a generalized inverse given by:

$$\tilde{G}^{-1}=C_{p_0}G^{\mathrm{T}}(C_{d_0}+GC_{p_0}G^{\mathrm{T}})^{-1}=(G^{\mathrm{T}}C_{d_0}^{-1}G+C_{p_0}^{-1})G^{\mathrm{T}}C_{d_0}^{-1}.\tag{5b}$$

$G[\mathbf{p}(\mathbf{r})]$ is the Frechet derivative of the operator $\mathbf{g}$ at the point $\mathbf{p}(\mathbf{r})$, and G^{T} is the adjoint of $\mathbf{G}$. C_{d_0} is the covariance matrix of data. C_{p_0} is the *a priori* covariance function on parameters at points $\mathbf{r}$ and $\mathbf{r}'$. C_{p_0} describes the *a priori* confidence in the *a priori* model $\mathbf{p}_0(\mathbf{r})$. There are two ways to check the reliability of the inversion: either by considering the *a posteriori* covariance function $C_p(\mathbf{r},\mathbf{r}')$ (Tarantola & Valette 1982) or for a linear problem by looking at the resolution $R(\mathbf{r},\mathbf{r}')$ (Montagner 1986a). C_p and R are defined as follows:

$$C_p=C_{p_0}-\tilde{G}^{-1}GC_{p_0}=(G^{\mathrm{T}}C_{d_0}^{-1}G+C_{p_0}^{-1})^{-1}\tag{6a}$$

$$R=\tilde{G}^{-1}G=C_p^{-1}G^{\mathrm{T}}C_{d_0}^{-1}G=C_{p_0}G^{\mathrm{T}}(C_{d_0}+GC_{p_0}G^{\mathrm{T}})^{-1}G.\tag{6b}$$

When this algorithm is expressed in its continuous form, the model $\mathbf{p}(\mathbf{r})$ is a multifunctional and the inverse problem is underdetermined. This approach is quite similar to that of Backus & Gilbert (1968, 1970). But in our case, the choice of an *a priori* covariance function on parameters is fundamental because it introduces a smoothing in the solution. In the continuous form, equations (5) and (6) are expressed by:

$$\begin{aligned}\mathbf{p}(\mathbf{r})-\mathbf{p}_0(\mathbf{r})=&\sum_{i=1}^{i=n_d}\sum_{j=1}^{j=n_d}\int_{\text{path}_i}C_{p_0}(\mathbf{r},\mathbf{r}_i)G_i^{\mathrm{T}}(\mathbf{p})\frac{ds_i}{\Delta_i}\\&\times(S_{ij}^{-1})\left(d_j-g_j(p)-\int_{\text{path}_j}G_j(p)[\mathbf{p}(\mathbf{r}_j)-\mathbf{p}_0(\mathbf{r}_j)]\frac{ds_j}{\Delta_j}\right)\end{aligned}\tag{7a}$$

$$\begin{aligned}C_p(\mathbf{r},\mathbf{r}')=&C_{p_0}(\mathbf{r},\mathbf{r}')-\sum_{i=1}^{i=n_d}\sum_{j=1}^{j=n_d}\int_{\text{path}_i}C_{p_0}(\mathbf{r},\mathbf{r}_i)G_i^{\mathrm{T}}(\mathbf{p})\\&\times\frac{ds_i}{\Delta_i}\int_{\text{path}_j}(S_{ij}^{-1})C_{p_0}(\mathbf{r}_j,\mathbf{r}')G_j(\mathbf{p})\frac{ds_j}{\Delta_j}\end{aligned}\tag{7b}$$

$$R(\mathbf{r},\mathbf{r}')=\sum_{i=1}^{n_d}\sum_{j=1}^{n_d}\int_{\text{path}_i}C_{p_0}(\mathbf{r},\mathbf{r}_i')G_i(\mathbf{p})\frac{ds_i}{\Delta_i}(S_{ij}^{-1})G_j(\mathbf{p})\frac{ds_j(\mathbf{r}')}{\Delta_j}\tag{7c}$$

$$S_{ij}=C_{d_{0ij}}+\int_{\text{path}_i}G_i(\mathbf{p})\frac{ds_i}{\Delta_i}\int_{\text{path}_j}G_j(\mathbf{p})\frac{ds_j}{\Delta_j}C_{p_0}(\mathbf{r},\mathbf{r}').$$

n_d is the number of data, $G_i(\mathbf{p})$ are the Frechet derivative of the operator $\mathbf{g}$ for parameter $\mathbf{p}$ at point $\mathbf{r}_i$ belonging to the path i. If the regionalization is restricted to the inversion of the $0\text{–}\Psi$ and $2\text{–}\Psi$ azimuthal distributions, $\mathbf{p}(\mathbf{r})$ is the 3-functional such that

$$\mathbf{p}^{\mathrm{T}}(\mathbf{r})=[A_1(\mathbf{r}),A_2(\mathbf{r}),A_3(\mathbf{r})]\quad\text{and}$$

$$G(\mathbf{p})=\left[\frac{-1}{V_0^2},\frac{-\cos 2\psi(\mathbf{r})}{V_0^2},\frac{-\sin 2\psi(\mathbf{r})}{V_0^2}\right].$$

The *a posteriori* covariance function $C_p(\mathbf{r},\mathbf{r}')$ and the resolution $R(\mathbf{r},\mathbf{r}')$ are 3×3 matrices, the elements of which are the different covariance functions or resolution functions expressing the correlation between the parameters. They are defined as follows:

$$C_p(\mathbf{r},\mathbf{r}')=\begin{bmatrix}C_{A_1A_1}(\mathbf{r},\mathbf{r}') & C_{A_1A_2}(\mathbf{r},\mathbf{r}') & C_{A_1A_3}(\mathbf{r},\mathbf{r}')\\ C_{A_2A_1}(\mathbf{r},\mathbf{r}') & C_{A_2A_2}(\mathbf{r},\mathbf{r}') & C_{A_2A_3}(\mathbf{r},\mathbf{r}')\\ C_{A_3A_1}(\mathbf{r},\mathbf{r}') & C_{A_3A_2}(\mathbf{r},\mathbf{r}') & C_{A_3A_3}(\mathbf{r},\mathbf{r}')\end{bmatrix}\tag{8a}$$

$$R(\mathbf{r},\mathbf{r}')=\begin{bmatrix}R_{A_1A_1}(\mathbf{r},\mathbf{r}') & R_{A_1A_2}(\mathbf{r},\mathbf{r}') & R_{A_1A_3}(\mathbf{r},\mathbf{r}')\\ R_{A_2A_1}(\mathbf{r},\mathbf{r}') & R_{A_2A_2}(\mathbf{r},\mathbf{r}') & R_{A_2A_3}(\mathbf{r},\mathbf{r}')\\ R_{A_3A_1}(\mathbf{r},\mathbf{r}') & R_{A_3A_2}(\mathbf{r},\mathbf{r}') & R_{A_3A_3}(\mathbf{r},\mathbf{r}')\end{bmatrix}.\tag{8b}$$

It is possible to assume that in the *a priori* covariance function $C_{A_iA_j}=0$ if $i\neq j$ (which means no correlation between velocity and azimuthal anisotropy). We find easily from (6a) and (6b) the different covariance functions

$C_{p_ip_j}$ and $R_{p_ip_j}$. For instance, for C_p

$$C_p = C_{p_0} - \begin{bmatrix} C_{A_1A_1}G_{A_1}^{\mathrm{T}}S^{-1}G_{A_1}C_{A_1A_1} & C_{A_1A_1}G_{A_1}^{\mathrm{T}}S^{-1}G_{A_2}C_{A_2A_2} & C_{A_1A_1}G_{A_1}^{\mathrm{T}}S^{-1}G_{A_3}C_{A_3A_3} \\ C_{A_2A_2}G_{A_2}^{\mathrm{T}}S^{-1}G_{A_1}C_{A_1A_1} & C_{A_2A_2}G_{A_2}^{\mathrm{T}}S^{-1}G_{A_2}C_{A_2A_2} & C_{A_2A_2}G_{A_2}^{\mathrm{T}}S^{-1}G_{A_3}C_{A_3A_3} \\ C_{A_3A_3}G_{A_3}^{\mathrm{T}}S^{-1}G_{A_1}C_{A_1A_1} & C_{A_3A_3}G_{A_3}^{\mathrm{T}}S^{-1}G_{A_2}C_{A_2A_2} & C_{A_3A_3}G_{A_3}^{\mathrm{T}}S^{-1}G_{A_3}C_{A_3A_3} \end{bmatrix}. \quad (9)$$

The physical meaning of C_p and R are not very different and they are related by the relation:

$$C_p(\mathbf{r}_1, \mathbf{r}_3) = [\delta(\mathbf{r}_1, \mathbf{r}_2) - R(\mathbf{r}_1, \mathbf{r}_2)]C_{p_0}(\mathbf{r}_2, \mathbf{r}_3).$$

For a well-resolved problem, $R = \delta(\mathbf{r}_1, \mathbf{r}_2)$ which is similar to the resolving kernel of Backus & Gilbert (1970) whereas $C_p(\mathbf{r}_1, \mathbf{r}_3) = 0$. C_p and R express the trade-off between the different distributions of parameters $A_1(\mathbf{r})$, $A_2(\mathbf{r})$, $A_3(\mathbf{r})$ and for a given couple of parameters p_i and p_j, $C_{p_ip_j}$ and $R_{p_ip_j}$ provides the lateral trade-off between two points. As can be seen from the relations (8), the final covariance function or resolution of parameters are dependent at the same time upon the theory through the kernels and also upon the quality of the dataset through the number of data and the covariance matrix of data. Some examples of the calculation of C_p are presented in the next paper (Montagner & Jobert, this issue).

SENSITIVITY OF SURFACE WAVE ANISOTROPY TO PETROLOGICAL MODELS

In long-period seismology, there is no *a priori* knowledge of the combinations $B_{c,s}$, $G_{c,s}$, $H_{c,s}$, $E_{c,s}$ defined previously by equations (2) and we do not know which constraints could be brought to bear on these parameters in an inversion process. And it seems important to see if geology, petrology or mineralogy enables us to reduce the space of parameters. Since Hess (1964) demonstrated the azimuthal dependence of P_n velocities in oceanic areas, the evidence that much of the upper mantle may be anisotropic is steadily increasing. The origin of this anisotropy has long been debated and the reader is referred to a special issue of the *Geophysical Journal of the Royal Astronomical Society* (Crampin, Chesnokov and Hopkin 1984) or to the review paper of Estey, Douglas & Spetzler (1986). It can reasonably be assumed that large-scale anisotropy in the upper mantle is due to crystallographic alignment of intrinsically anisotropic minerals, mainly olivine and pyroxenes (Estey & Douglas 1986). Different petrological studies of ophiolites (Christensen 1984; Peselnick & Nicolas 1978) have shown that the fast axis of olivine-rich aggregates tends to align in the flow direction whereas the intermediate and slow axes are more dispersed, giving a fast 'unique' axis.

Montagner & Nataf (1986) calculate these different combinations for the elastic tensor evaluated by Peselnick & Nicolas (1978) from field observations of an ophiolite complex in Turkey. They find that the two important contributions to long-period surface wave azimuthal anisotropy come from B and G. The first one has a shallow influence whereas the second one has a deeper influence. Kawasaki & Kon'no (1984) proposed a model of the possible form of constituent olivine which is axisymmetric about the fast axis in the uppermost mantle beneath the Pacific Ocean. Cara & Lévêque (1987) can explain multimode surface waves by introducing a percentage of oriented olivine down to 400 km. Estey & Douglas (1986) constrained the real earth anisotropy by the limits of maximum anisotropy from perfect mineral alignment. They found that the anisotropy of the upper mantle as described by PREM (Dziewonski & Anderson 1981) down to 220 km is best represented by the pryolite model (Ringwood 1975) which reduces to quasi-hexagonal symmetry. Below 220 km, the piclogite model with an orthorhombic symmetry (Anderson & Bass 1984) is preferred.

In this section, we consider the elastic coefficients and their pressure and temperature dependence as given in table 1 of Estey & Douglas (1986). We compute the different combinations defined by (2) as well as $\frac{(A-C)}{C}$, $\frac{(N-L)}{L}$ for olivine, pyrolite, piclogite and also for the experimental sample of Peselnick & Nicolas (1978; hereafter P & N) (Table 1). The coordinates system has been chosen so as to align the *a*-axis (fast axis) along the 1-axis and the *b*-axis (slow axis) along the 3-axis except for piclogite. In this system of coordinates, the 1-axis is the flow direction, the plane defined by the 1- and 2-axis is the flow plane. Now instead of coordinates related to mineralogy or a convection process, we prefer coordinates attached to the earth. The horizontal plane is defined by the 1-axis and 2-axis, the 1-axis being the direction of maximum P-velocity in this plane; the 3-axis is the vertical one. As the flow direction is not necessarily vertical or horizontal, we have rotated the *a*-, *b*- and *c*- axes so as to explore the variation range of P-wave anisotropy, S-wave anisotropy, B and G combinations. In Fig. 3, different diagrams show

Table 1. Anisotropic elastic moduli and P and T derivatives. (After Estey & Douglas 1986.)

C_{ij} (Mbar/100)	olivine	pyrolite	piclogite	P & N
C_{11}	323.7	269.0	248.0	236.58
C_{12}	71.6	54.8	59.2	72.5
C_{13}	66.4	63.1	75.9	72.3
C_{22}	235.1	200.0	202.8	220.8
C_{23}	75.6	66.7	72.1	71.9
C_{33}	197.6	197.5	219.1	220.2
C_{44}	64.6	69.8	75.7	74.9
C_{55}	79.0	78.3	78.7	79.2
C_{66}	78.05	79.7	81.9	78.8
A	266.5	229.4	224.9	229.0
C	197.6	197.5	219.1	220.2
F	71.0	64.9	74.0	72.1
L	71.8	74.1	77.2	77.1
N	91.0	84.8	82.5	78.4
B	44.3	34.5	22.6	7.8
G	7.2	4.3	1.5	2.1
H	−4.6	−1.8	1.9	0.2
C'	12.9	5.1	0.6	−0.4
ε	34.7	0.9	−12.8	−3.3
$(A-C)/C$ %	34.9	16.2	26.2	4.0
$(N-L)/L$ %	26.7	14.5	6.9	1.7

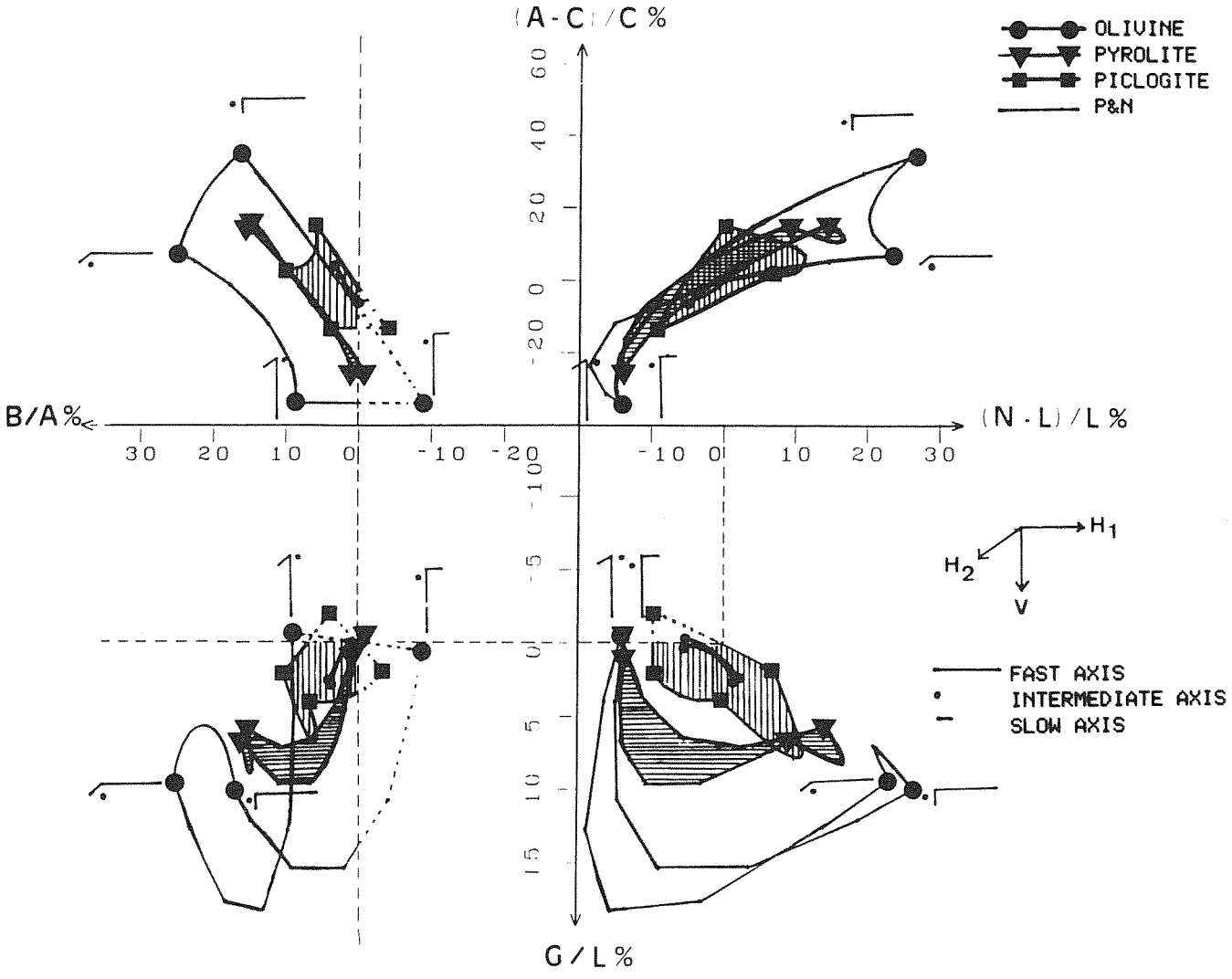

Figure 3 Variation at shallow depth of $\frac{A-C}{C}$ (related to P-wave anisotropy) with respect to $\frac{N-L}{L}$ (related to S-wave anisotropy) and $\frac{B}{A}$ (related to P-wave 2ψ-azimuthal anisotropy) and of $\frac{G}{L}$ (related to S-wave 2ψ-azimuthal anisotropy) with respect to $\frac{N-L}{L}$ and $\frac{B}{A}$. This representation in four quadrants allows a quick comparison of the variation ranges of these different observable forms of anisotropy for olivine, the experimental sample of Peselnick & Nicolas (1978) and for two petrological models (pyrolite and piclogite).

simultaneously the variations of P-wave anisotropy $\left(\text{through } \frac{A-C}{C}\right)$, S-wave anisotropy $\left(\text{through } \frac{N-L}{L}\right)$, 2ψ-azimuthal anisotropy in the P-wave $\left(\text{through } \frac{B}{C}\right)$ and the S-wave $\left(\text{through } \frac{G}{L}\right)$. The *a*-, *b*- and *c*-axes are plotted when they are coincident with the Cartesian coordinates. The long dashed line '——' corresponds to the *a*-axis, the small one '—' to the *b*-axis and the dot '.' to the *c*-axis.

Let us consider the upper right quadrant where the P-wave anisotropy $\frac{A-C}{C}$ is plotted with respect to the S-wave anisotropy $\frac{N-L}{L}$. The domains of the different minerals overlap one another, the variation range being maximum for olivine. All the domains include the experimental sample of Peselnick & Nicolas (1978). If we look at the variation of $\frac{B}{A}$ (P-wave 2ψ-azimuthal anisotropy) with respect to $\frac{A-C}{C}$, the different domains are still imbricated. But if we look at the lower right quadrant in which $\frac{G}{L}$ (S-wave 2ψ-azimuthal anisotropy) is plotted with respect to $\frac{N-L}{L}$, the different domains are separated. Therefore, S-wave azimuthal anisotropy (through the G-combination) seems to be very sensitive to the mineralogical composition. However, our calculations assume a perfect alignment and in order to describe a more

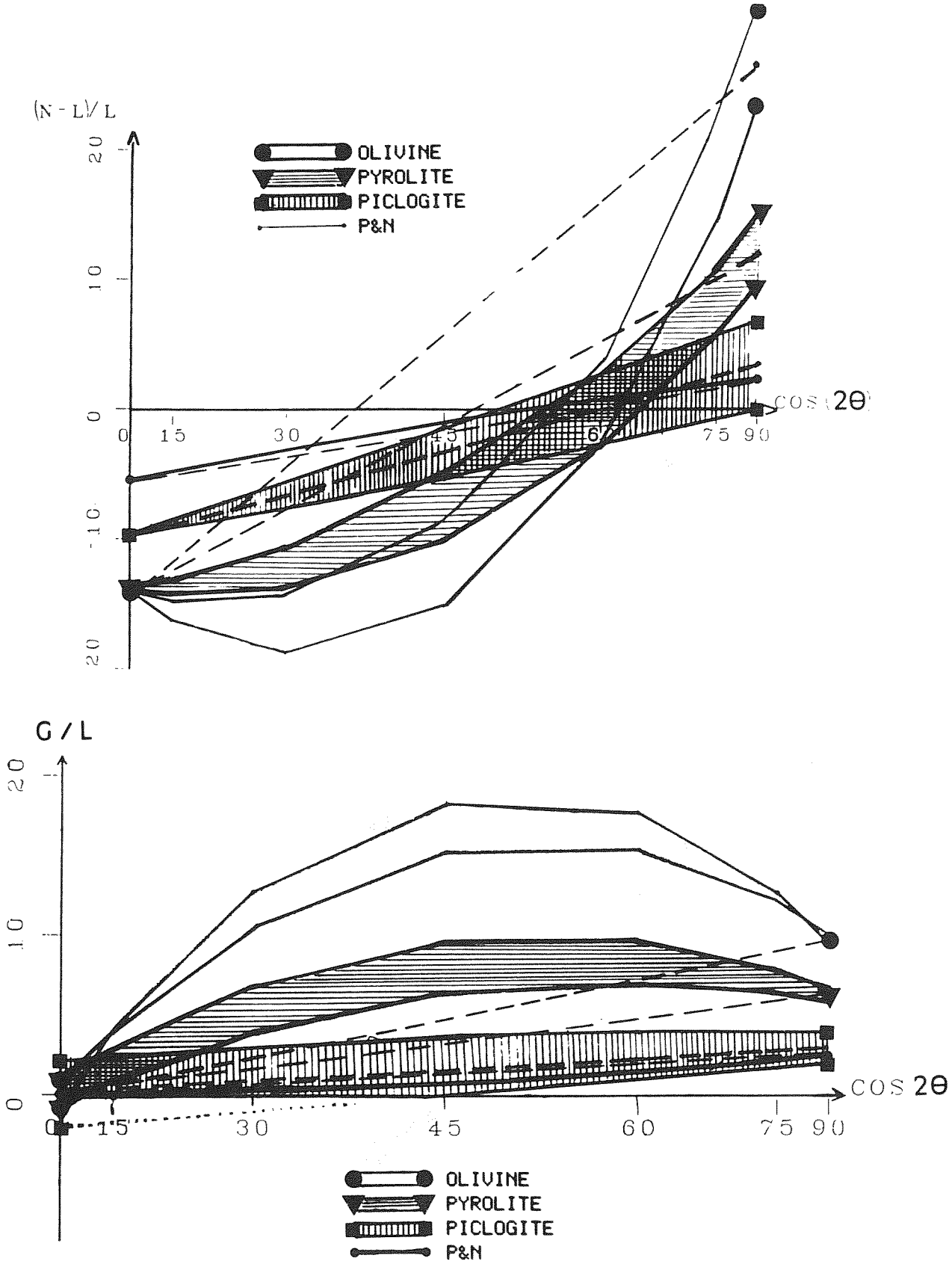

Figure 4 (a) Variation of $\frac{N-L}{L}$ (S-wave anisotropy) with respect to $x = \cos 2\theta$ (where θ is the vertical orientation of the symmetry axis) (b): $\frac{G}{L}$ with respect to x.

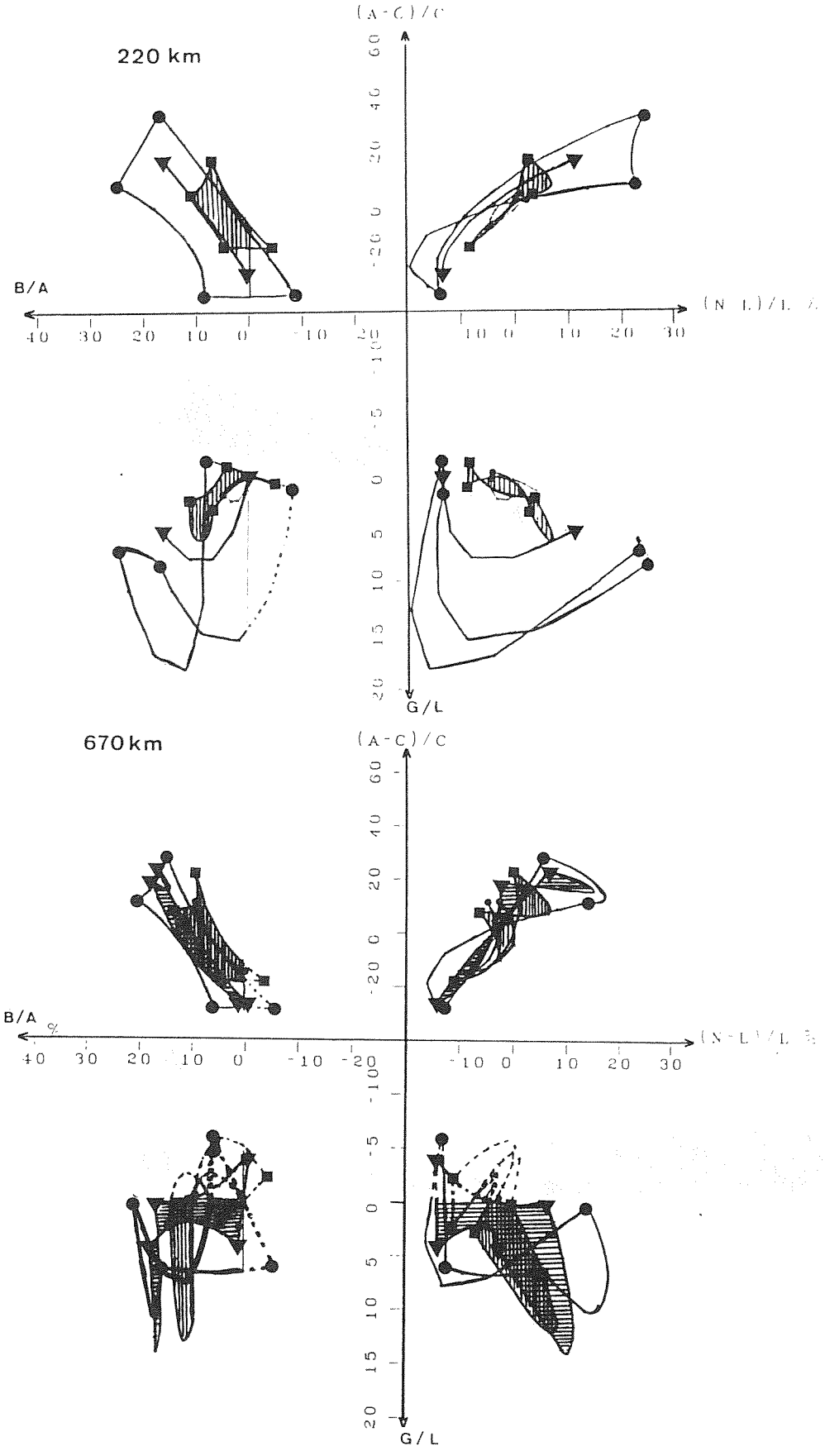

Figure 5 Same as Fig. 3 for two other depths: (a) 220 km. (b) 670 km.

realistic earth, it is necessary to investigate the effect of a probability distribution or the effect of a proportion of randomly orientated crystals. If random orientation exists, the different domains will have a tendency to be closer to zero and the actual domains of variation include the area between 0 and the extreme bounds of the domains (Montagner & Anderson 1987). Of course, any interpretation must take account of this effect, because according to the diagram giving $\frac{G}{L}$ as a function of $\frac{N-L}{L}$, we should conclude that piclogite best explains the results of Peselnick & Nicolas (1978). However, we must bear in mind that it can be explained by pyrolite with some random orientation or probability distribution.

On the other hand, it can be noted that for a medium axisymmetric about the fast axis (called orthotropic medium later on), the domains reduce to continuous lines because two of the three axes are now randomly orientated in the plane perpendicular to the symmetry axis. Montagner & Anderson (1987) investigate in a systematic way the effect of random orientation on the different combinations defined by formula (2). It can be seen that P & N and to some degree, pyrolite fulfil this condition of axisymmetry about the fast axis (equivalent to orthotropy) and their B and G combinations are little dependent on the orientations of the slow and intermediate velocity axes. Therefore, for pyrolite and P & N the hypothesis of orthotropy is quite justified. It is not the case for piclogite which has a very broad variation of domains. However, these calculations assume a perfect alignment which is presumably true at small scale but not at a large scale. As noted previously, in ophiolite sections (Christensen 1984), the orientation of the fast axes of olivine along the flow direction and the random orientation of the b- and c-axes give a fast symmetry axis for olivine at the scale of a massif. Therefore, in the real case, picolgite is probably more orthotropic than could be inferred from these calculations. This symmetry axis of the orthotropic medium can be defined by two angles: an azimuth Ψ and an orientation with respect to vertical θ. In Fig. 4, we have plotted $\frac{N-L}{L}$ and $\frac{G}{L}$ with respect to $x = \cos 2\theta$. It can be seen that two values of θ may correspond to a given value of $\frac{N-L}{L}$ or $\frac{G}{L}$. Therefore, the variation of the anisotropic parameters as a function of θ is non-linear. In the next section, we will see that this non-linearity is related to a combination ϵ, itself related to the combination E present in the 4ψ-azimuthal terms. The difference between the linear case (dashed line) and the real computation is important for olivine and also to a less extent for pyrolite but small for piclogite and P & N (Fig. 4). If we consider the linear case, the angle θ will be overestimated, but as the non-linearity is not too large for the actual case of P & N, a first approximation for the angle θ can be obtained by the linear equations.

Those calculations were performed under the assumption that the pressure, P and temperature T are those of the Earth surface. Now we make use of the partial derivatives of C_{ij} with respect to P and T (Estey & Douglas 1986) and plot the same diagrams as Fig. 3 for two different depths 220 and 670 km. The temperature profile comes from Stacey (1977) and the pressure variation with depth comes from the PREM model of Dziewonski & Anderson (1981). There is no difference between the diagrams of Fig. 3 and Fig. 5a (220 km) but the striking feature is that the pyrolite domain reduces now to a continuous line which means that pryolite is axisymmetric about the fast axis at this depth. At a depth of 670 km, (Fig. 5b), all the domains seem to be intertwined and have complex boundaries. It is likely that at this depth, the P and T partial derivatives are imprecise and the precision of the extrapolation poor. Moreover, phase transformations of the different constituents are not taken into account. However, bearing in mind these limitations we can see that the correlation between P-wave and S-wave anisotropy still holds at this depth.

Therefore, the main conclusions of this section are the following:

(i) $\frac{A-C}{C}$ and $\frac{N-L}{L}$ which express the anisotropy of respectively P-wave and S-wave in a transversely isotropic medium with a vertical symmetry axis are correlated in the whole upper mantle. This kind of constraint can be used in an inversion process.

(ii) The B and G combinations are less correlated and G which is the most sensitive to the mineralogical composition, could be used as a discriminant between petrological models.

(iii) Pyrolite and P & N are quite orthotropic but not piclogite for perfect alignment. But petrological considerations suggest that the approximation of orthotropy is correct.

(iv) When the orientation θ of the symmetry axis is looked for, non-linear terms which are only dependent on a combination ε will bias the determination of θ. But as ε is related to the combination E which can only be determined from 4ψ-azimuthal terms, this nonlinear effect is not easily corrected for. Therefore, the linear determination of θ must be seen as a first approximation of the actual orientation of the symmetry axis.

INTERPRETATION OF INVERTED COMBINATIONS IN TERMS OF AN ORTHOTROPIC MATERIAL

The different ingredients for the inversion of Rayleigh and Love dispersion data are now defined and we can theoretically retrieve the 13 combinations of elastic moduli given in relations (2). At this stage we did not make any assumption about the medium (except that anisotropy, if any, is small) but the next problem concerns the interpretation of these.

The number of these parameters is still too large to allow for a simple interpretation and moreover seismic data cannot resolve so many parameters. Therefore it seems necessary to decrease the number of parameters. The tendency of random orientation about the fast axis (Christensen 1984; Peselnick & Nicolas 1978) suggests that locally the medium possess a symmetry axis. In order to explain the azimuthal anisotropy this symmetry axis must be assumed to have any orientation. This kind of medium is called throughout the text an orthotropic medium. It can be described by seven parameters: A_0, C_0, F_0, L_0, N_0 and two

angles defining the symmetry axis: θ_0 and Ψ_0. θ_0 is the orientation of the symmetry axis with respect to the vertical and Ψ_0 is the azimuth of its horizontal projection (see Fig. 2). It must be pointed out that, as surface waves cannot distinguish Ψ_0 from $\Psi_0 + \pi$, the orientations θ_0 and $-\theta_0$ are also equivalent for surface wave propagation and we must not forget this intrinsic limitation in any interpretation of the symmetry axis. A_0, C_0, F_0, L_0 and N_0 can be defined for a reference medium in which the symmetry axis is vertical. It must be pointed out that the transverse isotropy is equivalent to the orthotropy such as it has been defined, but we prefer this last term because there is often confusion between transverse isotropy and transverse isotropy with a vertical symmetry axis (such as PREM for instance) which cannot explain azimuthal anisotropy. If we can retrieve the seven parameters of the orthotropic medium, a geodynamic interpretation can be undertaken in relating the symmetry axis to the flow direction in a convection process.

We must now relate the combinations A_R, C_R, F_R, L_R, N_R, B_R, G_R and E_R theoretically retrieved from surface wave dispersion, to the seven parameters of the orthotropic medium. We do not calculate these combinations with respect to Ψ_0 because it is always possible at a given depth to write:

$$\begin{aligned} B_c \cos 2\psi + B_s \sin 2\psi &= B \cos 2(\psi - \Psi_B) \\ G_c \cos 2\psi + G_s \sin 2\psi &= G \cos 2(\psi - \Psi_G) \\ H_c \cos 2\psi + H_s \sin 2\psi &= H \cos 2(\psi - \Psi_H) \\ E_c \cos 4\psi + E_s \sin 4\psi &= E \cos 4(\psi - \Psi_E). \end{aligned} \tag{10}$$

Table 2. (a) Elastic coefficients when the symmetry axis is vertical.

C	1	2	3	4	5	6
1	A_0	$A_0 - 2N_0$	F_0	0	0	0
2	$A_0 - 2N_0$	A_0	F_0	0	0	0
3	F_0	F_0	C_0	0	0	0
4	0	0	0	L_0	0	0
5	0	0	0	0	L_0	0
6	0	0	0	0	0	N_0

The elastic tensor coefficients γ_{ijkl} in the new coordinates system are obtained by rotating the reference frame according to the rule:

$$\gamma_{ijkl} = c_{npqr} m_{ni} m_{pj} m_{qk} m_{rl} \tag{11}$$

where m_{st} are the elements of the rotation matrix $\mathbf{M}$ given by:

$$\mathbf{M} = \begin{bmatrix} \cos\theta_0 \cos\Psi_0 & -\sin\Psi_0 & \sin\theta_0 \cos\Psi_0 \\ \cos\theta_0 \sin\Psi_0 & \cos\Psi_0 & \sin\theta_0 \sin\Psi_0 \\ -\sin\theta_0 & 0 & \cos\theta \end{bmatrix}.$$

When we perform such a rotation, it is better to consider the fourth-order elastic tensor c_{ijkl} than the simplified C_{ij} matrix. This parameterization of the medium (with seven unknowns) is the simplest way to create azimuthal anisotropy. It corresponds to a hexagonal symmetry but the unique axis is not radial. We give in Table 2 the relations Γ_{ij} and C_{ij} which were redefined in their simplified index notation, when the symmetry axis is rotated in the 1–3 plane by an angle θ_0 (see Fig. 2). The elastic combinations defined by formula (2) can be recalculated and the different $\cos^k \theta_0$, $\sin^k \theta_0$ can be developed as $\cos 2\theta_0$, $\sin 2\theta_0$, $\cos 4\theta_0$, $\sin 4\theta_0$. We give now the different combinations A_R, C_R, F_R, L_R, N_R, B_R, G_R, H_R and E_R which correspond to the orthotropic medium in the direction θ_0. 0ψ-term:

$$\begin{aligned} A_R = {} & \frac{A_0}{64}(41 + 20\cos 2\theta_0 + 3\cos 4\theta_0) \\ & + \frac{C_0}{64}(9 - 12\cos 2\theta_0 + 3\cos 4\theta_0) \\ & + \frac{F_0 + 2L_0}{32}(7 - 4\cos 2\theta_0 - 3\cos 4\theta_0) \end{aligned}$$

$$\begin{aligned} C_R = {} & \frac{A_0}{8}(3 - 4\cos 2\theta_0 + \cos 4\theta_0) \\ & + \frac{C_0}{8}(3 + 4\cos 2\theta_0 + \cos 4\theta_0) + \frac{F_0 + 2L_0}{4}(1 - \cos 4\theta_0) \end{aligned}$$

(b) Elastic coefficients when the symmetry axis is rotated in the plane 1–3 by an angle Θ.

γ	1	2	3	4	5	6
1	$A_0 \cos^4\theta + C_0 \sin^4\theta + (2F_0 + 4L_0)\cos^2\theta \sin^2\theta$	$(A_0 - 2N_0)\cos^2\theta \sin^2\theta + F_0 \sin^2\theta$	$(A_0 + C_0 - 4L_0)\cos^2\theta \sin^2\theta + F_0(\cos^4\theta + \sin^4\theta)$	0	$A_0 \cos^3\theta \sin\theta - C_0 \cos\theta \sin^3\theta$	0
2	γ_{12}	A_0	$(A_0 - 2N_0)\sin^2\theta + F_0 \cos^2\theta$	0	$(A_0 - 2N_0 - F_0)\cos\theta \sin\theta$	0
3	γ_{13}	γ_{23}	$A_0 \sin^4\theta + C_0 \cos^4\theta + (2F_0 + 4L_0)\cos^2\theta \sin^2\theta$	0	$(A_0 - 2L_0 - F_0)\sin^3\theta \cos\theta + (F_0 + 2L_0 - C_0)\cos^3\theta \sin\theta$	
4	0	0	0	$N_0 \sin^2\theta + L_0 \cos^2\theta$	0	$(N_0 - L_0)\sin\theta \cos\theta$
5	γ_{15}	γ_{25}	γ_{35}	0	$(A_0 + C_0 - 2F_0)\sin^2\theta \cos^2\theta + L_0(\cos^2\theta - \sin^2\theta)$	0
6	0	0	0	γ_{46}	0	$N_0 \cos^2\theta + L_0 \sin^2\theta$

$$F_R = \frac{A_0}{16}(5 - 4\cos 2\theta_0 - \cos 4\theta_0) + \frac{C_0 + 4L_0}{16}(1 - \cos 4\theta_0) + \frac{F_0}{8}(5 + 2\cos 2\theta_0 + \cos 4\theta_0) + \frac{N_0}{2}(1 - \cos 2\theta_0)$$

$$L_R = \frac{A_0 + C_0 - 2F_0}{16}(1 - \cos 4\theta_0) + \frac{L_0}{4}(2 + \cos 2\theta_0 + \cos 4\theta_0) + \frac{N_0}{4}(1 - \cos 2\theta_0)$$

$$N_R = \frac{A_0 + C_0 - 2F_0}{64}(3 - 4\cos 2\theta_0 + \cos 4\theta_0) + \frac{L_0}{16}(5 - 4\cos 2\theta_0 - \cos 4\theta_0) + \frac{N_0}{2}(1 + \cos 2\theta_0)$$

2ψ term:

$$B_R = \frac{A_0}{16}(-5 + 4\cos 2\theta_0 + \cos 4\theta_0) + \frac{C_0}{16}(3 - 4\cos 2\theta_0 + \cos 4\theta_0) + \frac{F_0 + 2L_0}{8}(1 - \cos 4\theta_0)$$

$$G_R = \frac{A_0 + C_0 - 2F_0}{16}(1 - \cos 4\theta_0) + \frac{L_0}{4}(-\cos 2\theta_0 + \cos 4\theta_0) - \frac{N_0}{4}(1 - \cos 2\theta_0) \tag{12b}$$

$$H_R = \frac{A_0}{16}(-3 + 4\cos 2\theta_0 - \cos 4\theta_0) + \frac{C_0 - 4L_0}{16}(1 - \cos 4\theta_0) + \frac{F_0}{8}(1 - 2\cos 2\theta_0 + \cos 4\theta_0) + \frac{N_0}{2}(1 - \cos 2\theta_0)$$

4ψ term:

$$E_R = \frac{A_0 + C_0 - 2F_0 - 4L_0}{64}(3 - 4\cos 2\theta_0 + \cos 4\theta_0) \tag{12c}$$

It is assumed that the 1-axis is orientated according to the direction of maximum velocity. When $\theta_0 = 0$ we find the case of a transversely isotropic medium with a vertical symmetry axis. We can express equations (12) in a slightly different way by assuming that A_0, C_0, F_0, L_0 and N_0 are first-order pertrubations of isotropic Lame's coefficients λ and μ. In an isotropic medium, we have: $A = C = \lambda + 2\mu$, $F = \lambda$, $L = N = \mu$. It is always possible to choose another parameterization such that:

$$\begin{aligned} A_0 &= \lambda_{eq} + 2\mu_{eq} \\ C_0 &= A_0(1 - \pi) \\ F_0 &= \lambda_{eq}(1 - \gamma) \\ L_0 &= \mu_{eq} \\ N_0 &= \mu_{eq}(1 - \sigma). \end{aligned} \tag{13}$$

π is related to P-wave anisotropy, γ to η by the relation $\eta = 1 - \gamma$ and σ is related to S-wave anisotropy. To have a more compact notation, we set $x = \cos 2\theta_0$. By introducing these different transformations, we can rewrite (12) as:

$$A_R = A_0 - \frac{\pi A_0}{4}(1 - x) - \frac{\varepsilon}{32}(5 - 2x - 3x^2)$$

$$C_R = A_0 - \frac{\pi A_0}{2}(1 + x) - \frac{\varepsilon}{4}x^2$$

$$F_R = \lambda_{eq} - \frac{\pi A_0}{2}(3 - x) + \frac{L_0\sigma}{2}(1 - x) - \frac{\varepsilon}{8}(2 + x + x^2)$$

$$L_R = L_0 - L_0\frac{\sigma}{4}(1 - x) + \frac{\varepsilon}{8}(1 - x^2)$$

$$N_R = L_0 - L_0\frac{\sigma}{2}(1 + x) - \frac{\varepsilon}{32}(1 - 2x + x^2) \tag{14}$$

$$B_R = -\frac{A_0\pi}{4}(1 - x) - \frac{\varepsilon}{8}(1 - x^2)$$

$$G_R = L_0\frac{\sigma}{4}(1 - x) + \frac{\varepsilon}{8}(1 - x^2)$$

$$H_R = -\left(\frac{\pi A_0}{8} + \frac{L_0\sigma}{2}\right)(1 - x) + \frac{\varepsilon}{8}x(1 - x)$$

$$E_R = \frac{\varepsilon}{32}(1 - x)^2$$

where $\varepsilon = 2\lambda_{eq}\gamma - \pi A_0 = A_0 + C_0 - 2F_0 - 4L_0$.

We can see in these expressions that the x^2 terms depend only on the parameter ε. If we take account of ε, the third step, which consists in retrieving either A_0, C_0, F_0, L_0, N_0, θ_0 or λ, μ, π, σ, ε, θ_0 will not be linear. If the dataset allows for the determination of the five terms of the azimuthal expansion in equation (1) for Rayleigh and Love waves, then it is possible to invert for these six parameters. But if the dataset only allows for the determination of the constant terms and the 2ψ-azimuthal terms, it is not possible to invert for the E_R combination and, therefore, ε. Classically, two approaches exist: either only the parameters corresponding to the largest partial derivatives are inverted (Woodhouse & Dziewonski 1984; Tanimoto 1986a) or physical constraints are imposed on the different parameters (Nataf *et al.* 1984, 1986). In the first approach, we get a good resolution of the selected parameters but their amplitude variation may be biased and generally overestimated, whereas in the second approach, though more rigorous, the assessment of constraints is in general very difficult. In the next paper (this issue), we follow the first approach for simplicity and the selected parameters will be in this case L_0, N_0, G_c, G_s (or G and Ψ_G). However, the previous section showed that constraints between the complete set of parameters can be found for different petrological models and Montagner & Anderson (1987) give an extensive investigation of petrological constraints on seismic anisotropy which should allow us to pursue the second approach in the future.

We present now a simplification of the problem which enables us to explain a dataset of Rayleigh, Love, 0ψ and 2ψ azimuthal velocities. We neglect the variations of the density ρ and λ, π, ε. We recall that to neglect ε is equivalent to neglecting the combinations $E_{c,s}$ and that it is dictated mainly by data. We also neglect the variations of π and therefore B, because their partial derivatives influence is smaller than those of L, N and G. However, we must not forget the problem of trade-off between shallow P-wave velocities (or shallow B anisotropy) variations and deep

S-wave velocities (or deep G anisotropy) variations (Montagner & Nataf 1986) and some experiments can be performed to assess this trade-off. The system of equations (14) becomes very simple and can be written:

$$\begin{aligned} L_R &= L_0\left[1+\frac{\sigma}{4}(x-1)\right] & & & L_0 &= L_R + G_R \\ N_R &= L_0\left[1-\frac{\sigma}{2}(1+x)\right] & &\Leftrightarrow & \sigma &= \frac{L_R + 3G_R - N_R}{L_R + G_R} \\ & & \text{if} \quad L_R + 3G_R - N_R \neq 0 & & & \\ G_R &= L_0\frac{\sigma}{4}(1-x) & & & x &= \frac{L_R - G_R - N_R}{L_R + 3G_R - N_R} \\ \Psi_G &= \Psi_0 & & & \Psi_0 &= \Psi_G. \end{aligned} \tag{15}$$

In this case, the solution is very simple and can be considered as the starting point of a more accurate description of the medium. This analytical solution presents some interesting features. According to (17), x can be found larger than 1 or smaller than -1. If that is the case, we can attribute the value 1 to x with the appropriate sign. The study of the condition $|x| \leq 1$ provides three ranges for N_R, bearing in mind that G_R is always positive:

$$\begin{aligned} N_R < L_R + G_R &\Rightarrow |x| < 1 \Rightarrow & 0° < \theta_0 < 90° \\ L_R + G_R < N_R < L_R + 2G_R &\Rightarrow x < -1 \Rightarrow x = -1 & \theta_0 = 90° \\ N_R > L_R + 3G_R &\Rightarrow x > 1 \Rightarrow x = 1 & \theta_0 = 0°. \end{aligned}$$

This last condition may seem quite surprising because it means that, though $V_{SH} > V_{SV}$, the symmetry axis is vertical whereas this situation should be interpreted as horizontal symmetry axis (or horizontal flow) by considering only the constant terms of Rayleigh and Love azimuthal velocity expansions. As a matter of fact, this last interpretation is wrong because we must have also a correlative azimuthal anisotropy. The corollary of this third condition is that the anisotropy σ is negative which is not very easy to explain petrologically or geodynamically. The errors on data can give rise to this kind of extraordinary situation. Alternatively, the hypothesis of the existence of a symmetry axis may be too strong. This very simple analytical solution is well suited when we only have the 0ψ and 2ψ terms of the azimuthal expansion (1). Naturally, if we are able to obtain in addition the 4ψ azimuthal terms, it is possible to enhance our description of the elastic medium starting from equations (14).

CONCLUSIONS

We have detailed in this paper a complete technique to retrieve simultaneously lateral heterogeneities of seismic velocities $\mathbf{L_0(r)}$ and their anisotropies $\boldsymbol{\alpha}[\sigma(\mathbf{r}), \theta_0(\mathbf{r}), \Psi_0(\mathbf{r})]$ from the azimuthal expansion of surface wave velocities. The complete process was summarized in Fig. 1. According to the quality of the dataset, some simplifications can be used. In the hypothesis of an orthotropic medium, we show how to retrieve the characteristics of the symmetry axis (amplitude σ, angles θ_0, Ψ_0). This method can provide interesting information about the convection process in the mantle by indicating the three-dimensional flow directions but also a discrimination between petrological models. An application of the method is presented in the next paper (Montagner & Jobert, this issue).

ACKNOWLEDGMENTS

We acknowledge the Seismological Laboratory of the I.P.G. of Paris as a whole, and particularly Nelly Jobert, Georges Jobert, Raul Madariaga, Barbara Romanowicz, Genevieve Roult, Albert Tarantola and Bernard Valette. We also thank Claude Allegre, Michel Cara, Jean-Paul Poirier and Toshiro Tanimoto for fruitful discussions.
IPGP contribution No.

REFERENCES

Anderson, Don L. & Bass, J. D., 1984. Mineralogy and composition of the upper mantle, *Geophys. Res. Lett.*, **11,** 637–640.
Anderson, Don L. & Bass, J. D., 1986. Transition region of the Earth's upper mantle, *Nature*, **320,** 321–328.
Backus, G. E., 1965. Possible forms of seismic anisotropy of the upper mantle under oceans, *J. Geophys. Res.*, **70,** 3429–3439.
Backus G. E., 1970. A geometrical picture of anisotropic elastic tensors, *Rev. Geophys.*, **8,** 633–671.
Backus, G. E. & Gilbert, F., 1968. The resolving power of gross earth data, *Geophys. J. R. astr. Soc.*, **16,** 169–205.
Backus, G. E. & Gilbert, F., 1970. Uniqueness in the inversion of inaccurate gross earth data, *Phil. Trans. R. Soc. A*, **266,** 123–192.
Cara, M. & Lévêque, J. J., 1987. Orientated olivine crystals in the Upper mantle: a test from the inversion of multimode surface-wave data, *Phys. Earth Planet. Int.*, **47,** 246–252.
Christensen, N. I., 1984. The magnitude, symmetry and origin of upper mantle anisotropy based on fabric analyses of ultramafic tectonites, *Geophys. J. R. astr. Soc.*, **76,** 89–111.
Christensen, N. I. & Salisbury, M. H., 1979. Seismic anisotropy in the oceanic upper mantle, *J. geophys. Res.*, **84,** 4601–4610.
Crampin, S., 1970. The dispersion of surface waves in multilayered anisotropic media, *Geophys. J. R. astr. Soc.*, **21,** 387–402.
Crampin, S., Chesnokov, E. M. & Hipkin, R. G., 1984. Seismic anisotropy – the state of art: II, *Geophys. J. R. astr. Soc.*, **76,** 1–16.
Davis, J. P. & Henson, I. H., 1986. Validity of the great circular average approximation for inversion of normal mode measurements, *Geophys. J. R. astr. Soc.*, **85,** 69–92.

Dziewonski, A. M. & Anderson, Don L., 1981. Preliminary Reference Earth Model, *Phys. Earth Planet. Int.*, **25,** 297–356.
Edmonds, A. R., 1960. *Angular momentum in Quantum Mechanics,* Princeton University Press.
Estey, L. H. & Douglas, B. J., 1986. Upper mantle anisotropy: A preliminary model, *J. Geophys. Res.*, **91,** 11393–11406.
Estey, L. H., Douglas, B. J. & Spetzler, H., 1986. A synthesis for upper mantle: I. Anisotropy, *Rev. Geophys.*, submitted.
Hager, B. & O'Connell, R., 1979. Kinematic models of large-scale flow in the Earth's mantle, *J. Geophys. Res.*, **84,** 1031–1048.
Hess, H., 1964. Seismic anisotropy of the upper most mantle under the oceans, *Nature,* **203,** 629–631.
Jordan, T. H., 1978. A procedure for estimating lateral variations from low frequency eigenspectra data, *Geophys. J. R. astr. Soc.*, **52,** 441–455.
Kawasaki, I. & Kon'no, F., 1984. Azimuthal anisotropy of surface waves and the possible type of the seismic anisotropy due to preferred orientation of olivine in the uppermost mantle beneath the Pacific Ocean, *J. Phys. Earth,* **32,** 229–244.
Maupin, V., 1985. Partial derivatives of surface-wave phase velocities for flat anisotropic models, *Geophys. J. R. astr. Soc.*, **83,** 379–398.
Mitchell, B. J., 1984. On the inversion of Love- and Rayleigh-wave dispersion and implications for the Earth structure and anisotropy, *Geophys. J. R. astr. Soc.*, **76,** 233–241.
Mochizuki, E., 1986. The free oscillations of an anisotropic and heterogeneous Earth, *Geophys. J. R. astr. Soc.*, **86,** 167–176.
Montagner, J. P., 1986a. Regional three-dimensional structures using long-period surface waves, *Ann. Geophys., 4,* **B3,** 283–294.
Montagner, J. P., 1986b. First results on the three-dimensional structure of the Indian Ocean inferred from long-period surface waves, *Geophys. Res. Lett.*, **13,** 315–318.
Montagner, J. P. & Anderson, Don L., 1987. Petrological constraints on anisotropy, *Phys. Earth Planet. Int.*, submitted.
Montagner, J. P. & Jobert, N., 1988. Vectorial Tomography. II: Application to the Indian Ocean, *Geophys. J. R. astr. Soc.*, **94,** 309–344.
Montagner, J. P. & Nataf, H. C., 1986. A simple method for inverting the azimuthal anisotropy of surface waves, *J. Geophys. Res.*, **91,** 511–520.
Nataf, H. C., Nakanishi, I. & Anderson, Don L., 1984. Anisotropy and shear-velocity heterogeneities in the upper mantle, *Geophys. Res. Lett.*, **11,** 109–112.
Nataf, H. C., Nakanishi, I. & Anderson, Don L., 1986. Measurements of mantle wave velocities and inversion for lateral heterogeneities and anisotropy. Part III: Inversion, *J. Geophys. Res.*, **91,** 7261–7307.
Nicolas, A. & Poirier, J. P., 1976. *Crystalline plasticity and solid state flow in metamorphic rocks,* John Wiley, New York, 437 pp.
Peselnick, L. & Nicolas, A., 1978. Seismic anisotropy in an ophiolite peridotite. Application to oceanic upper mantle, *J. Geophys. Res.*, **83,** 1227–1235.
Phinney R. A. & Burridge, R., 1973. Representation of the elastic gravitational excitation of a spherical earth model by generalized spherical harmonics, *Geophys. J. R. astr. Soc.*, **34,** 451–487.
Ringwood, A. E., 1975. Composition and petrology of the Earth's mantle, McGraw-Hill, New York, 618 pp.
Schlue, J. W. & Knopoff, L., 1977. Shear-wave polarization anisotropy in the Pacific Ocean, *Geophys. J. R. astr. Soc.*, **49,** 145–165.
Smith, M. L. & Dahlen, F. A., 1973. The azimuthal dependence of Love and Rayleigh wave propagation in a slightly anisotropic medium, *J. Geophys. Res.*, **78,** 3321–3333.
Stacey, F. D., 1977. A thermal model of the Earth, *Phys. Earth Planet. Int.*, **15,** 341–348.
Suetsugu, D. & Nakanishi, I., 1985. Surface wave tomography for the upper mantle beneath the Pacific ocean. Part I: Rayleigh wave phase velocity distribution, *J. Phys. Earth,* **33,** 345–368.
Tanimoto, T., 1986a. The Backus–Gilbert approach to the 3-D structure in the upper mantle. II: SH and SV velocity, *Geophys. J. R. astr. Soc.*, **84,** 49–69.
Tanimoto, T., 1986b. Free oscillations in a slightly anisotropy Earth, *Geophys. J. R. astr. Soc.*, **87,** 493–517.
Tanimoto, T. & Anderson, Don L., 1984. Mapping convection in the mantle, *Geophys. Res. Lett.*, 287–290.
Tanimoto, T. & Anderson, Don L., 1985. Lateral heterogeneity and azimuthal anisotropy of the upper mantle: Love and Rayleigh waves 100–250 s, *J. Geophys. Res.*, **90,** 1842–1858.
Tarantola, A. & Valette, B., 1982. Generalized nonlinear inverse problems solved using the least squares criterion, *Rev. Geophys. Space Phys.*, **20,** 219–232.
Woodhouse, J. H. & Dziewonski, A. M., 1984. Mapping the upper mantle: Three dimensional modelling of Earth structure by inversion of seismic waveform, *J. Geophys. Res.*, **89,** 5953–5986.